Supramolecular Recognition: Protonmotive-Driven Switches or Motors?

James D. Crowley, Andrew J. Goshe, Ian M. Steele, and Brice Bosnich*[a]

Abstract: A dicationic molecular receptor bearing two cofacially disposed terpyridyl-Pd-Cl units forms stable 1:1 host–guest complexes with planar, neutral platinum(II) complexes. When the guest is modified to incorporate a pyridine group, the now basic guest is protonated by trifluoroacetic acid in acetonitrile solutions. The basic yellow guest forms a stable, deep red 1:1 host–guest complex with the yellow palladium receptor. Addition of trifluoroacetic acid to this host–guest complex leads to the displacement of the guest from the receptor. It is proposed that the dissociation of the guest is caused by electrostatic repulsion between the dicationic receptor and the positively charged protonated guest. Addition of base restores the host–guest complex. This protonmotive translocation of the guest from the host to the solution is discussed in terms of the mechanisms that drive molecular motors, the power stroke and the Brownian ratchet. It is concluded that the system is best described as a molecular switch that operates by the same mechanism as one stroke of a molecular motor

Keywords: host–guest systems · molecular motors · molecular switches · protonmotive displacement · supramolecular chemistry

Introduction

It has become common to refer to certain responses of supramolecular assemblies as representing the operation of molecular switches, motors, or even machines. How the response of a molecular assembly to various chemical or physical stimuli is characterized can depend on the perspective of the observer of the phenomena. Since we deal with the operation of what are described as molecular switches or motors herein, it is useful to define these terms. Although there are more complicated definitions,[1] a simple molecular switch can be defined as a molecular system that can be induced to transform from one state to another by stimuli such as light, electrochemistry, or chemical reactions. Changes in state are, of course, associated with changes in physical characteristics. A molecular motor is a molecular assembly that can transform chemical energy into mechanical work. Molecular motors, therefore, involve the coupling of chemical reactions with molecular motion and usually refer to molecular assemblies where concerted, repetitive chemically driven "strokes" cause specific molecular movement. A molecular machine is a molecular motor that uses its work for a specific task, such as locomotion. These definitions imply that a molecular switch and motor can operate in a similar manner if the switch involves molecular translocation.

Biological systems incorporate numerous molecular motors that perform a variety of tasks.[2] Relevant in the present context are the rotary molecular motors, F_oF_1ATPase[3] and the bacterial flagella motor[4] that are driven by the protonmotive force associated with transmembrane proton gradients. In the former case, motor rotation leads to ATP synthesis whereas in the latter the protonmotive force driven rotation leads to bacterial locomotion. The mechanism by which the molecular motion is driven by the proton gradient is complex, but relies on electrostatic, hydrophobic, and hydrophilic interactions that are switched on and off by protonation and deprotonation.[3] The biological rotary motors are especially complex machines so that attempts to emulate some of their features in simple systems present formidable challenges. Despite this, a number of reports have appeared of systems that couple chemical energy with molecular motion.[5] In the present context, two examples of proton promoted translocation are notable. One of these is a two-site rotaxane that, upon protonation of the rotaxane thread, leads to intramolecular site translocation of the charged, threaded macrocycle.[6] An intermolecular analogue involves a positively charged platinum-based host bearing dimethylaniline guests.[7] In this case the guests are released from the positively charged host cavity by guest protonation. In both of these examples the host–guest association arises from weak noncovalent forces[8] that are overcome by elec-

[a] J. D. Crowley, Dr. A. J. Goshe, Dr. I. M. Steele, Prof. B. Bosnich
Department of Chemistry, The University of Chicago
5735 South Ellis Avenue, Chicago, IL 60637 (USA)
Fax: (+1) 773-702-0805
E-mail: bos5@uchicago.edu

Supporting information for this article is available on the WWW under http://www.chemeurj.org/ or from the author.

DOI: 10.1002/chem.200305620

trostatic repulsion after protonation. The work described here examines several aspects of proton-induced guest dissociation from host–guest complexes. The process is discussed in terms of the work that is done.

Results and Discussion

Host–guest complexes: In previous work[9] we showed that the palladium-based receptor **1** forms a very stable 1:1 association complex with the platinum complex **2**. It was found

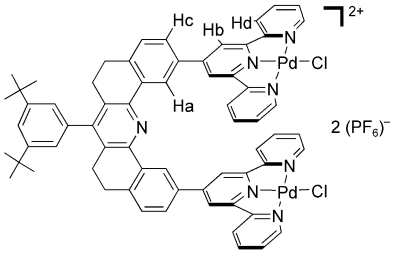

1

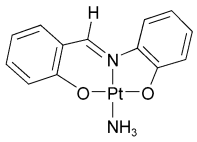

2

both in solution and in the solid state that the guest **2** lies within the molecular cleft provided by the receptor **1**, and is probably stabilized by π–π stacking interactions and by weak metal–metal interactions between the host and guest metals.[10] Although the host–guest complex is stable in solution in CH_3CN, $K = 12\,000\ M^{-1}$, rapid intermolecular host–guest exchange occurs.

Because the receptor **1** is positively charged, a neutral guest in the cleft upon becoming positively charged, by some method, will experience strong electrostatic repulsion and consequently is expected to be repelled from the cleft into the solvent. The simplest method of switching the guest charge from neutral to positive is by using a neutral guest that can be protonated. Analogous guests to **2** are the platinum complexes **3**–**5**. The guests **3** and **4** are basic but **5** is

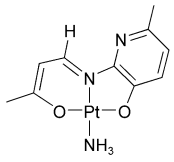

3

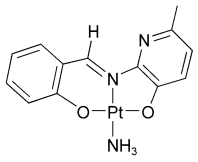

4

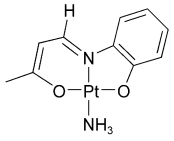

5

not. The 5-methyl groups were incorporated to hinder coordination of the pyridine nitrogen atom to metals. In the cases of **3** and **5**, formylacetone rather than acetylacetone was used to prepare the tridentate ligands to obtain planar complexes. When acetylacetone is used, the inner methyl group sterically interacts with the neighboring aromatic ring to cause the coordinated ligand to twist.[11] Such twisting would diminish the binding capacity of such guests in the cleft.

Crystal structures of 1 and 5: That the guest **5** is planar was established by its crystal structure (Figure 1, Table 1). The

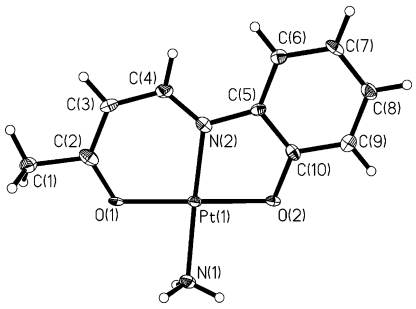

Figure 1. Structure of the guest **5** (ORTEP diagram; the thermal ellipsoids are shown at the 50% probability).

Table 1. Crystallographic data for **5** and **1**·5 CH_3CN.

Compound		**5**	**1**
formula		$C_{10}H_{12}N_2O_2Pt$	$C_{55}H_{55}Cl_2N_7Pd_2 + 2PF_6 + 5C_2H_3N$
formula weight		387.31	1713.07 (including solvent)
space group		$P2_1/c$	$P\bar{1}$
a [Å]		12.787(3)	13.169(3)
b [Å]		4.4830(10)	13.686(3)
c [Å]		18.885(4)	22.240(4)
α [°]		90.00	87.57(3)
β [°]		109.115(4)	85.34(3)
γ [°]		90.00	72.79(3)
V [Å^3]		1022.9(4)	3815.5(13)
Z		4	2
crystal size [mm], color, habit		0.68 × 0.60 × 0.80, orange, needle	0.07 × 0.04 × 0.015, yellow, diamond fragment
ρ_{calcd} [g cm^{-3}]	2.515	1.491	
μ [mm^{-1}]		13.697	0.663
T [K]		100(5)	100(5)
wavelength [Å]	0.71073	($Mo_{K\alpha}$)	0.54993 (synchrotron radiation)
$R(F)$ [%][a]		3.54	5.52
$R(wF^2)$ [%][a]		9.14	14.50

[a] Quantity minimized $= R(wF^2) = \Sigma[w(F_o^2 - F_c^2)^2]/\Sigma[(wF_o^2)^2]^{1/2}$; $R = \Sigma\Delta/\Sigma(F_o)$, $\Delta = |(F_o - F_c)|$, $w = 1/[\sigma^2(F_o^2) + (aP)^2 + bP]$, $P = [2F_c^2 + \mathrm{Max}(F_o, 0)]/3$.

average deviation of any non-hydrogen atom from the molecular plane is 0.07 Å. The bond lengths and angles are unexceptional and are provided in the Supporting Information.

Suitable crystals of **1** for structure determination using synchrotron radiation were grown from a solution in acetonitrile at −20 °C after standing for two years in a screw-top vial. The structure is shown in Figure 2 and the crystallographic data are provided in Table 1. It will be seen that the terpy-Pd-Cl units of pairs of molecules interpenetrate. A center of inversion lies between Pd(1A) and Pd(1B), and the spacer units are in chiral conformations, the molecules having opposite absolute configurations. The unit cell has two molecules of **1** as shown, but "vertical" stacking of terpy-Pd-Cl units extends through the crystal. This stacking is shown in Figure 3, in which the interplanar separations are given and interplanar angles are shown in brackets. The planes of the terpy-Pd-Cl units are essentially parallel and the interplanar distances within the unit cell are similar to those expected for π–π stacking. The planar separation between unit cells (Pd(2A), Pd(2B)) is larger than that expect-

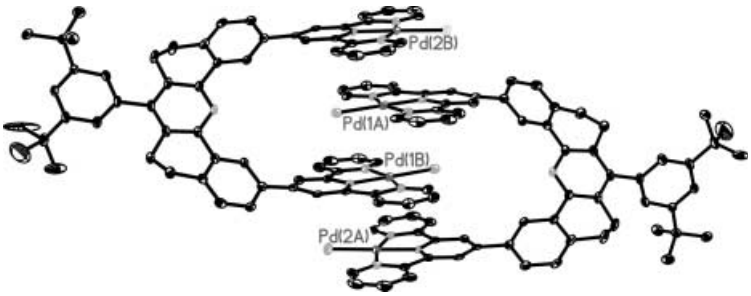

Figure 2. Side view of the stacking that is present in the crystal of **1**·5 CH_3CN (ORTEP diagram; thermal ellipsoids are shown at 50% probability). The solvent and counterions have been removed for clarity.

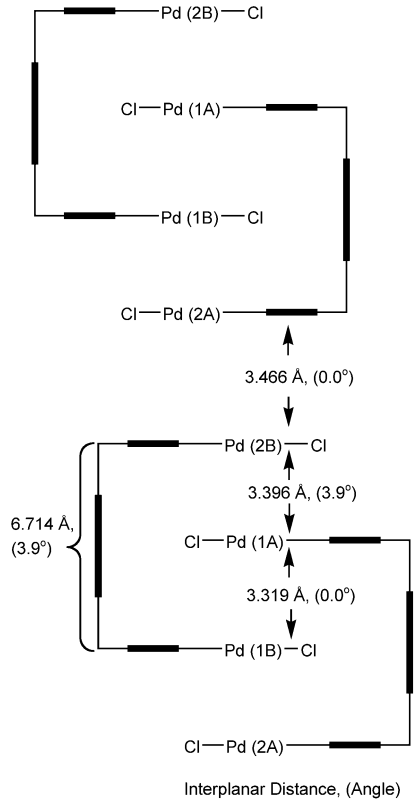

Figure 3. Representation of the stacking of the terpy-Pd-Cl units in the crystal of **1**·5 CH_3CN. The interplanar distances are given and the interplanar angles are shown in parentheses.

ed for π–π stacking. The terpy-Pd-Cl units of each molecule **1** are twisted with respect to the spacer, the planes are roughly parallel (3.9°) and are separated by 6.714 Å. The Pd–Pd distances depend on the interplanar separations and on the amount of displacement of these planes with respect to each other. Thus the interplanar separations do not necessarily reflect the metal–metal separations: Pd(1A)–Pd(1B) 3.364, Pd(1B)–Pd(2A) 3.453, Pd(2A)–Pd(2B) 4.471, and Pd(1A)–Pd(2A) 6.765 Å. The distance between Pd(1A) and Pd(1B) is the only separation that may indicate significant Pd–Pd interaction.[10]

The interpenetrated structure of **1** (Figure 2) must generate strong electrostatic repulsions between the closely spaced positively charged terpy-Pd-Cl units. In the crystal, the negatively charged PF_6^- counterions are found to cluster about the terpy-Pd-Cl units to neutralize the charges. Charged polypyridyl-Pd-X^+ complexes are known to stack in the solid state so that the interpenetrated structure found here is analogous.[12]

In acetonitrile solutions, **1** is completely dissociated. Thus, between 10^{-2} and 10^{-5} M the ^{1}H NMR spectrum and the absorption spectrum in the ultraviolet and visible regions are independent of concentration. Further, the conductivity of **1** in acetonitrile solutions is 235 $\Omega^{-1}cm^2mol^{-1}$ indicating that at 10^{-3} M, **1** is a 2:1 electrolyte.[13] Thus, the receptor **1** is fully dissociated with respect to itself and its counterions in acetonitrile solutions. Consistently, neither the terpy-Pd-Cl^+ nor the terpy-Pt-Cl^+ complex associates with **1** in acetonitrile solutions as judged from the ^{1}H NMR spectra and UV/Vis spectra.

Synthesis: The preparation of **1** is given elsewhere.[9] The preparation of **4** is outlined in Scheme 1. The nitro compound **6** is cleanly reduced to the air-sensitive amine **7** by the hydrazine/graphite[14] method and the Schiff's base **8** forms readily with salicylaldehyde. The platinum compound **9** is prepared by a variation of the Pregosin method.[15] Replacement of the dimethyl sulfoxide (DMSO) ligand from **9** by ammonia gives the ammine complex **4** efficiently.

The condensation of **7** with **10** to give **11** proved troublesome [Eq. (1)]. After all of the obvious solution methods were tried, simply heating a mixture of **7** and **10** provided the desired product **11** in reasonable yield and purity. The compound **11** is susceptible to ready hydrolysis. Reaction of

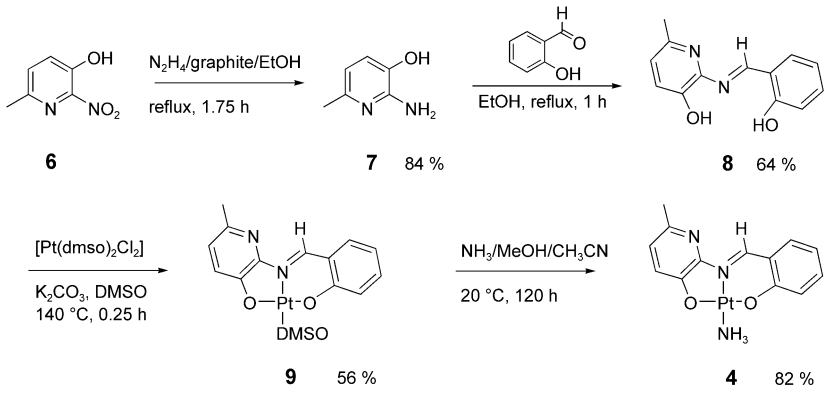

Scheme 1. Synthesis of **4**.

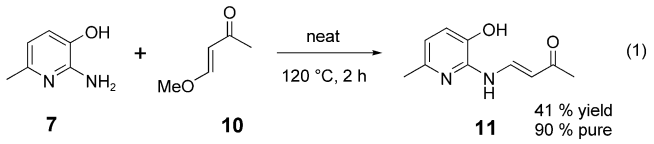

7 10 11

11 with $[Pt(dmso)_2Cl_2]$ by the method shown in Scheme 1 gives the DMSO complex that is then converted to the stable ammine complex **3.** The preparation of **5** followed a similar procedure except that, in this case, **10** reacted readily with *o*-aminophenol.

Host–guest formation: Solutions of the receptor **1** and of the potential guests **3**–**5** in acetonitrile are light yellow. Upon mixing of **1** with any one of these guests, a deep red solution results indicating host–guest formation. At 25 °C the ^{1}H NMR spectra of the three host–guest complexes **1** and **3**, **1** and **4**, **1** and **5** are broad but become sharp at 70 °C. The host–guest association constants for **1** and **3** and for **1** and **4** were determined in CD_3CN at 70 °C by the chemical shift titration method.[16] Both systems form 1:1 host–guest association complexes. The equilibrium constant for the host–guest complex between **1** and **3** is $K_{1,3}=21\,000\pm 4000\,\text{M}^{-1}$ and for the complex between **1** and **4** is $K_{1,4}=37\,000\pm 6000\,\text{M}^{-1}$. ESI-MS ($CH_3CN$) data for solutions containing **1** and **3**, **1** and **4**, as well as **1** and **5** also show that 1:1 host–guest complexes are formed and the mass spectra show isotopic resolution (see Supporting Information). The ^{1}H NMR spectra of the host–guest complexes show large chemical shifts for the H_a, H_b, and H_d protons (see **1**) of the receptor but almost no shift is observed for H_c. This indicates[17] that the guests reside inside of the molecular cleft and that they have essentially no residency time on the "outside" terpy-Pd-Cl face as is observed in other host–guest complexes.[9] This assertion is supported by the crystal structure of the host–guest complex between **1** and **3**.

X-ray data were collected on the adduct formed by **1** and **3** which was isolated by vapor diffusion of methanol into a host–guest solution in methyl ethyl ketone. It was found that the guest existed in two orientations in the ratio of 70:30 inside of the receptor cleft. Both orientations had the ammine ligands oriented in a similar direction as the two chloro groups of the receptor which has terpy-Pd-Cl units twisted with respect to each other. The two orientations of the guest are believed to arise from 180° rotation about the Pt–NH_3 bond. Because of the two orientations of the guest, we were unable to determine accurately the coordinates of all of the atoms of the guest molecule. The structure of the host–guest complex, as far as could be determined, is given in the Supporting Information. Several important features of the structure were determined with confidence, however. The three planes provided by the guest and two terpy-Pd-Cl units of the receptor are essentially parallel and the three metal atoms Pd-Pt-Pd are essentially aligned. The salient structural information is illustrated in Figure 4. The rather short Pt–Pd distances may indicate metal–metal interaction[10] and the interplanar separations are those expected for π-stacked molecules.

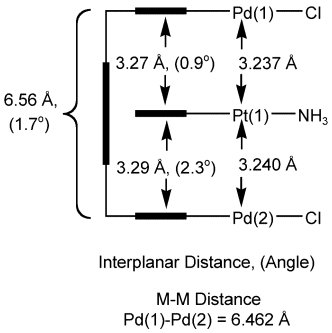

Figure 4. Schematic representation of the important structural details from the crystal structure of the host–guest complex formed from **1** and **3**.

Acid–base reactions: For the study of the protonation of the host–guest complexes, trifluoroacetic acid (TFA) was used because it was found that TFA readily protonated the free guest **3** in acetonitrile solution and that excess of TFA did not lead to decomposition of the guest nor the host over several hours at 70 °C. The pK_a values of the trifluoroacetic acid and pyridine in dry CH_3CN solution at 25 °C are reported[18] to be 12.65 and 12.33, respectively. Presumably, the free guests **3** and **4** in acetonitrile will have similar pK_a values to pyridine. The receptor **1**, however, also has a pyridine nitrogen atom, which could be protonated by TFA. The analogous pyridine compound **12** is reported[19] to have a pK_a of 1.73 in 70 % EtOH/H_2O at 25 °C. The lower than expected pK_a value may be due to the restricted cavity in which the nitrogen lone pair exists. A 10^{-3} M CD_3CN solution of **1** at 25 °C gave ^{1}H NMR spectra that were unchanged for up to 100 equivalents of TFA, suggesting that no protonation occurs. In addition to steric crowding, the very low pK_a of the receptor **1** in CD_3CN solution is probably connected with the electrostatic repulsions that are generated between the dipositively charged receptor and a positively charged protonated nitrogen atom of the receptor.

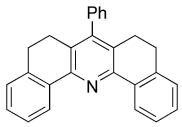

12

When considering the degree of dissociation of the guests **3** and **4** from their host–guest complexes in the presence of acid, three equilibria require consideration: the host–guest association constant K_{HG}, the dissociation constant of TFA, K_a, and the proton dissociation constant of the free guest, K_g. The constants are defined as shown in Scheme 2.

Combining these three equilibrium equations, an analytic expression for the relationship between the concentration of the host–guest complex with acid concentration can be derived (see supporting information). Further, using the expression for K_a and K_g, the variation of a physical property, such as optical density or chemical shift, with acid titration

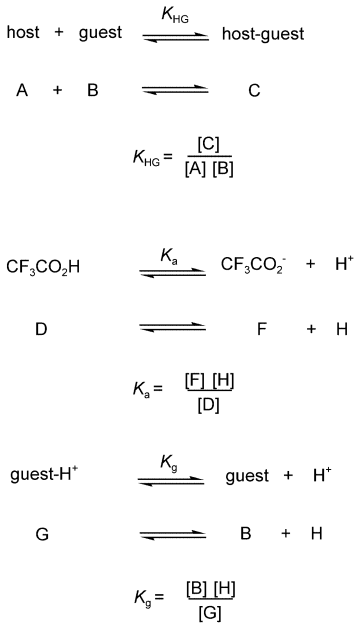

Scheme 2. Definition of the dissociation constants.

of the base can be derived analytically (see Supporting Information). In principle, the (real) solution of this equation will give the values of K_a and K_g. Knowing K_{HG} experimentally, it is possible in principle to find the concentration of all of the species in solution for a given acid concentration from the derived equations. In the present case, the pK_a values for TFA and **3** are likely to be about 12, in acetonitrile solution at 25 °C, but the most dilute concentration of guest that can be used for accurate physical measurements is 10^{-4} M. Under these circumstances, it is not possible to obtain accurate values of K_a and K_g from acid titration of the guest.[20]

Given these restrictions to the formal method, a different approach was used for assessing the amount of acid required to fully protonate the guest and for complete acid-induced dissociation of the guest from the host. The method involves plotting the variation in a physical property versus acid concentration. At the point where no further variation in physical property with acid concentration is observed, it is assumed that the guest is fully protonated or fully dissociated from the host.

Figure 5 shows the variation of the absorption spectrum of **3** upon incremental additions of dry TFA in dry CH_3CN solution at 25 °C. As will be noted, the spectral variation indicates that a clean protonation occurs. Figure 6 shows two plots of the change in absorbance versus equivalents of TFA derived from the data in Figure 5. Both plots indicate that the guest is fully protonated after about 20 equivalents of TFA are added. Figure 7 shows the variation in absorption spectra of the host–guest complex formed between **1** and **3** with added TFA. The absorption centered around 525 nm is the "charge transfer" absorption associated with host–guest formation. Upon successive additions of TFA to the host–guest complex, this band gradually decreases in intensity and at sufficient TFA the charge transfer band is extinguished. For most of the TFA addition, an isosbestic point is ob-

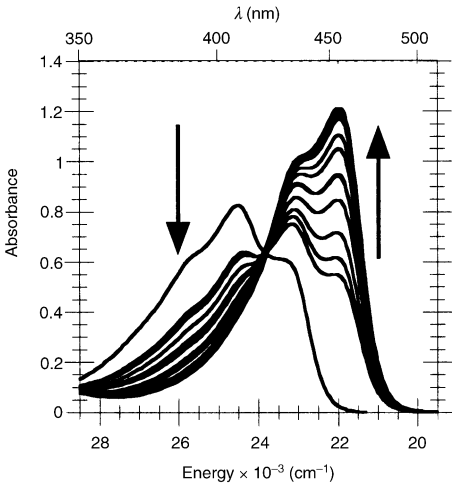

Figure 5. Absorption spectra for the titration of **3** with TFA. The experiments were performed at 25 °C in dry CH_3CN where the concentration of **3** was held constant at 0.477 mM and the concentration of TFA was varied between 0.927 mM and 38.9 mM.

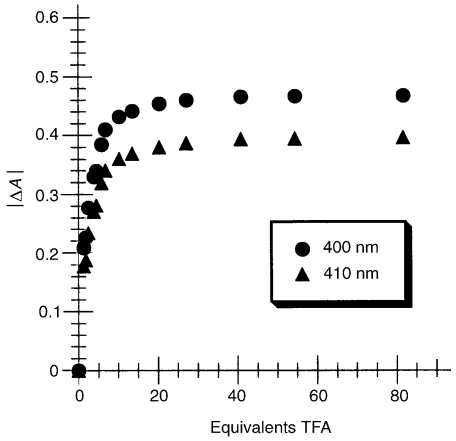

Figure 6. Plots of the absolute change in absorbance ($|\Delta A|$) versus equivalents TFA for the titration of **3** with TFA. The data is derived from Figure 5.

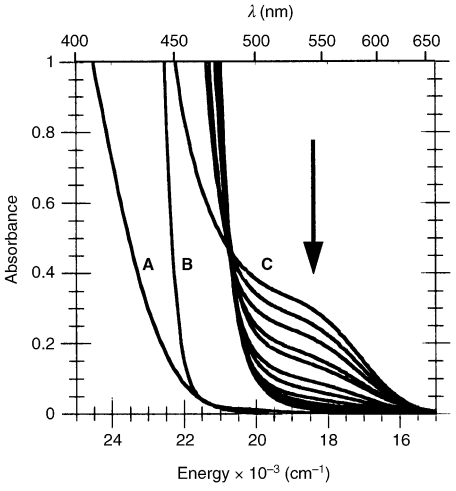

Figure 7. Absorption spectra for **1** (**A,** 2.00 mM), **3** (**B**, 2.00 mM), a 1:1 solution of **1** and **3** (**C**, 2.00 mM each), and the titration of the host–guest complex formed from **1** (2.00 mM) and **3** (2.00 mM) with TFA (varied between 4.62 mM and 191 mM). The experiments were performed at 25 °C in dry CD_3CN.

served. At nearly complete protonation of the guest (see Figure 5) the protonated guest has absorption which intrudes into the isosbestic point region. Visually, the solution of the host–guest complex changes from a deep red color to a light straw color as TFA is added. When triethylamine is incrementally added to the yellow solution derived from protonation of the guest in the host–guest solution, the variation of the spectrum in Figure 7 occurs in the reverse direction. When the number of equivalents of triethylamine is equal to the equivalents of TFA originally added, the host–guest spectrum is fully restored. Plots of the change in absorbance versus equivalents of TFA are shown in Figure 8

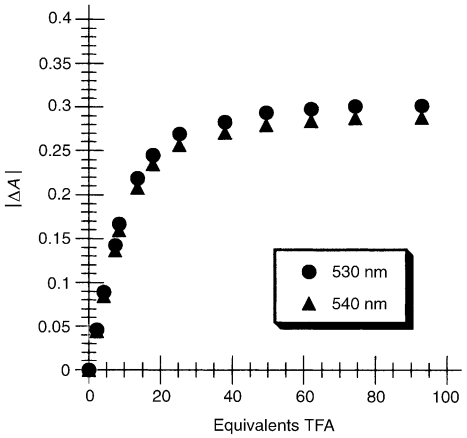

Figure 8. Plots of the absolute change in absorbance ($|\Delta A|$) versus equivalents TFA for the titration of the host–guest complex formed from **1** and **3** with TFA. The data is derived from Figure 7.

where it can be seen that about 45 equivalents of TFA are required to fully dissociate the guest **3**. The greater number of equivalents of TFA required to fully protonate the guest **3** in the presence of one equivalent of host **1** is due to competition for the guest by the host and the acid as defined by the equilibrium constants H_{HG}, K_a, and K_g. Titration of the guest **3** and the host–guest complex between **1** and **3** with TFA in dry CD_3CN solution at 70 °C was also monitored by ^1H NMR spectroscopy that showed shifts in the proton resonance frequencies in both the host and the guest upon guest protonation (see Supporting Information). Plots of chemical shifts versus TFA equivalents revealed similar stoichiometries as were observed from the UV data at 25 °C. The latter are more accurate, however.

The changes in physical property when the guest is allowed to react with TFA could arise from a guest–TFA hydrogen bonded adduct or from the formation of a separated protonated guest cation and trifluoroacetate anion. If the latter is the case, conductivity measurements should detect the formation of ions. The conductivity of the guest **3** alone and of TFA alone in dry acetonitrile at 25 °C is essentially zero. When dry TFA is added to a 10^{-3} M solution of **3** in dry CH_3CN solution, the molar conductivity increases until about 20 equivalents of TFA are added, which is the same saturation level found by spectrophotometry. At this concentration of TFA, the molar conductance was 110 $\Omega^{-1}\,cm^2\,mol^{-1}$. This conductance is somewhat lower than that expected for a 1:1 electrolyte in CH_3CN solution (120–160 $\Omega^{-1}\,cm^2\,mol^{-1}$)[13] but the observed conductivity indicates that protonated **3** and trifluoroacetate exist predominantly as separated ions in dilute CH_3CN solution. This observation supports the assertion that the guest in the presence of TFA exists as a positively charged ion that is expected to be repelled by the dicationic host **1**.

The guest **5** has no conventional basic elements and, consistently, addition of TFA to a solution of **5** in CH_3CN led to very small changes in the absorbance at around 400 nm indicating that some interaction between TFA and **5** may exist. As expected, the host–guest complex formed by **1** and **5** was not significantly affected by the addition of 100 equivalents of TFA as judged from absorption spectral changes.

The (basic) guest **4** forms a more stable host–guest complex with **1**, than does **3** with **1**. On this basis, alone, more TFA would be required to fully remove the guest from the host by protonation. More TFA would also be required if, in addition, **4** is a weaker base than **3**. This appears to be the case as seen from TFA titration of **4**, monitored by the absorption spectrum. The variation in the spectra with TFA addition, however, did not provide stable isosbestic points, suggesting that protonation generates more than one species. The overall spectra of the protonated and unprotonated guest **4**, however, was similar to those found for the guest **3** (Figure 4). Plots of absorbance versus equivalents of TFA at 25 °C in dry CH_3CN solution indicate that about 60 equivalents of TFA were required to fully protonate **4**, three times the number of equivalents of TFA required to fully protonate **3**. Thus **4** appears to be a weaker base than **3**, and **4** forms a more stable adduct with **1** than does **3**. Consistently, even after 200 equivalents of TFA were added to the host–guest complex, the guest **4** was not fully dissociated from the host **1**, as judged by spectrophotometry at 25 °C (Supporting Information).

Discussion

The proton-induced (protonmotive) dissociation of the guest from the receptor can be described in several ways. It can be referred to as an acid-induced shift in equilibrium, or as a molecular switch or as a molecular motor. Each and all of these descriptions are correct but each characterization elicits a different perspective on the process. The process described here is in some ways different from a conventional shift in equilibrium because the host–guest complex is stabilized by noncovalent forces and the guest is released from the host by noncovalent electrostatic forces. Because the protonmotive force causes the guest to move from the cleft of the receptor to the solution and the process is accompanied by a color change from red to yellow, the response of the system can be called a simple molecular switch. Because acid (or base) causes the translocation of the guest, the process can also be regarded as a single step (stroke) of a molecular motor. If the present system is described as one stroke of a molecular motor, it is necessary to demonstrate that work is done. This is shown by considering the mechanisms by which molecular motors operate.

Two distinct mechanisms are recognized that drive a molecular motor, the power stroke[21] and the Brownian ratchet.[22] Both mechanisms may operate in the same motor. These two mechanisms are illustrated in Scheme 3 and Scheme 4 for the present system. The power stroke is perhaps the simplest process to comprehend because it bears some relationship to the operation of macroscopic motors. The Brownian ratchet mechanism, however, bears no macroscopic motor analogy because it operates by the rectification of stochastic Brownian motion, that is, thermal energy is harnessed to do work.

Scheme 3 outlines the potential operation of the power stroke in the present system. The host–guest complex, **13**, is stabilized by noncovalent interactions. Because TFA is essentially undissociated in acetonitrile solution and because the receptor is a dication, it is unlikely that a solvated proton will exist to combine with the basic guest in the molecular cleft. It is more probable that TFA will form the neutral hydrogen bonded species, **14**, from which, upon release of the trifluoroacetate anion, the unstable host–guest complex **15** is generated. Electrostatic repulsion between the host and the protonated guest will lead to dissociation resulting in the formation of the free receptor **1** and the free protonated guest. The electrostatic force that operates on both the dication receptor and the protonated guest leads to molecular motion and, consequently, work (force by distance) is done on both the receptor and the guest.

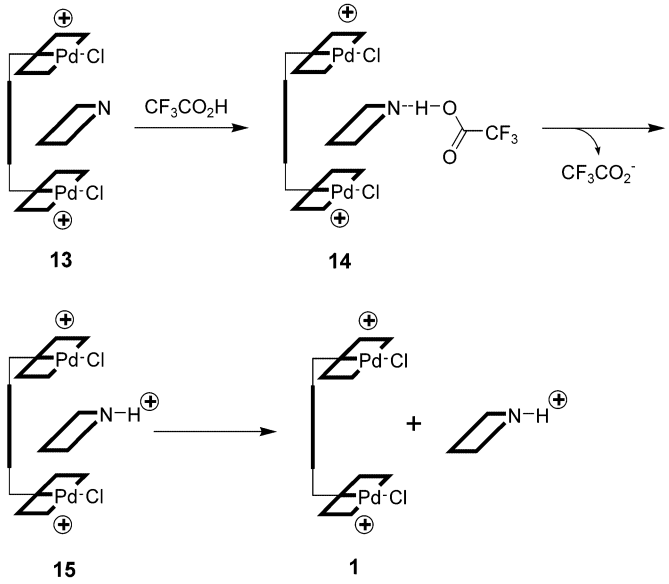

Scheme 3. Power stroke mechanism for driving a molecular motor.

The operation of the Brownian ratchet for the present system is illustrated in Scheme 4. Brownian motion induces (reversible) dissociation of the guest from the host–guest complex **13**. The free guest is then protonated by the acid and thus the guest is prevented from returning to the receptor. An alternative possible path involves the formation of the hydrogen-bonded host–guest complex **14**, followed by the dissociation of the hydrogen bonded guest which, by dissociation of trifluoroacetate, gives **1** and the protonated guest. As for the case of the power stroke, work is done in the Brownian ratchet mechanism because the protonated guest is unable to return to the receptor.

The experiments described here do not speak in support of one or other of these processes. It is probable, however, that both mechanisms participate for the present system. The proton induced translocation of the macrocycle in the two-site rotaxane[6] can be described by the mechanisms presented here. The acid-induced removal of dimethylanilines from the cationic platinum-based cage,[7] however, most probably involves the Brownian ratchet mechanism because strong acid in water was used. It is unlikely that protons would enter the positively charged cage to protonate an incarcerated guest.

If a molecular switch operates by translocation of a molecule, as is the case for the present protonmotive removal of the guest from the receptor, then one stroke of a switch is identical to one stroke of a motor. Consequently, whatever mechanism or description is ascribed to one can be ascribed to the other. Both require work to be performed on molecules.

One crucial aspect of molecular motors is that they are driven by a repetitive succession of molecular events, each of which does work and, in concert, leads to motion of molecular assemblies. For example, the proton driven motor, F_oF_1ATPase, has a rotor that has 9–14 protein copies[23] each of which is involved in a concerted unidirectional rotation of the rotor and its attached drive shaft.[24] Thus, if concerted

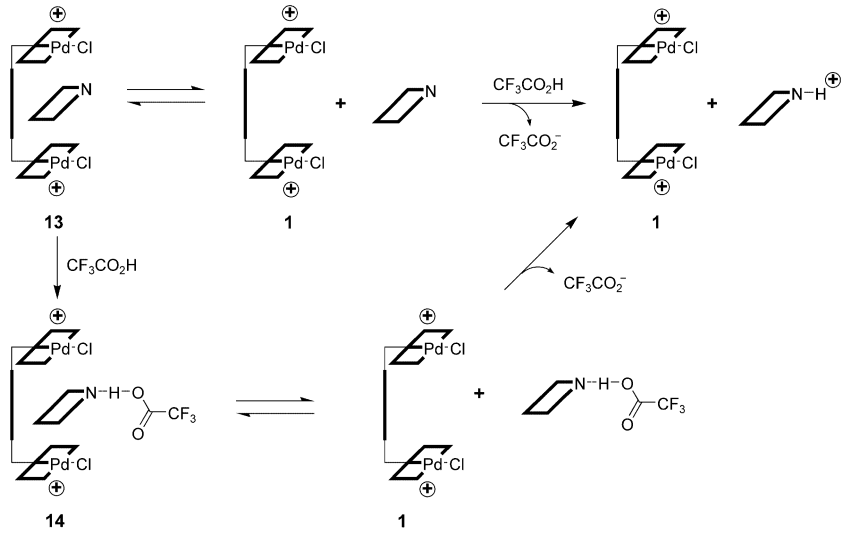

Scheme 4. Brownian ratchet mechanism for driving a molecular motor.

repetitive action is part of the definition of a molecular motor, the present and previously published chemically driven systems[5,25] are not motors. They are better described as molecular switches. But as noted here, the mechanisms for the operation of a molecular switch when molecular translocation is involved and of one stroke of a molecular motor can be the same. The difference is largely related to the function that the molecular device performs. Devising molecular systems that can drive a molecular assembly by concerted, repetitive strokes is a considerable challenge[26] but is a prerequisite to the development of molecular machines.

Conclusion

It has been shown that a dicationic receptor incorporating a neutral basic guest will release the guest upon guest protonation. Electrostatic repulsion is believed to cause host–guest dissociation, a process that is accompanied by a color change from deep red to yellow. It is suggested that the proton-driven dissociation of the guest can be described as a molecular switch or one stroke of a molecular motor. Both the switch and motor operate by similar mechanisms, namely, an electrostatically driven power stroke and a Brownian ratchet. Because molecular motors are usually defined as systems that operate by repetitive cycles, it is concluded that the present system is better described as a molecular switch.

Experimental Section

General procedures: All reagents were obtained from commercial suppliers and were used without further purification. All reactions were performed under an atmosphere of argon, unless otherwise specified. ^{1}H and ^{13}C NMR spectra were recorded using a Bruker DRX500 or a Bruker DMX500 Fourier transform spectrometer. Proton and carbon chemical shifts, δ, are reported in ppm, and referenced to tetramethylsilane (TMS). Coupling constants, J, are reported in hertz. Electronic absorption spectra were obtained using a Perkin Elmer Lambda 6 UV/Vis spectrophotometer. For a given wavelength and acid concentration, the absolute change in absorbance, ($|\Delta A|$), was calculated by subtracting the acid dependent absorbance from the absorbance in the absence of acid, ($|\Delta A|_o$). The absolute change in chemical shift, ($|\Delta A|_0$) is calculated similarly. Elemental analyses were performed by Desert Analytics, Tucson, Arizona. Conductance measurements were performed at 23 °C with 1×10^{-3} M samples using an YSI Scientific model 35 conductance meter. Melting points are uncorrected. Acetonitrile was dried over CaH_2, tetrahydrofuran (THF) was dried over potassium/benzophenone ketyl, diethyl ether was dried over sodium/benzophenone ketyl, and dichloromethane was dried over CaH_2. Dry trifluoroacetic acid (TFA) was obtained by distillation from a solution containing 5% trifluoroacetic anhydride. Thin layer chromatography was carried out using precoated silica gel (Whatman PE SIL G/UV) or precoated aluminum oxide (J. T. Baker, aluminum oxide IB-F). Silica gel 60 Å (Merck, 230–400 mesh) and aluminum oxide 58 Å (either activated, basic, Brockman I or activated, neutral, Brockman I) were used for chromatography as indicated. Celite is J.T. Baker Celite 503. [Pt(dmso)$_2$Cl$_2$] was prepared by the literature method.[27] The preparation of the receptor complex **1** has been previously described.[9]

2-Amino-6-methylpyridin-3-ol (7): A 100-mL flask was charged with the nitropyridine **6** (2.5 g, 16.22 mmol) dissolved in anhydrous ethanol (27 mL). Graphite (4.9 g) was added to this yellow solution. The flask was flushed with argon and hydrazine monohydrate (1.6 g, 1.6 mL, 32.44 mmol) was added. Upon addition of the hydrazine, the color of the exothermic reaction solution changed to bright yellow and the viscosity of the suspension increased. The suspension was stirred for 5 min whereafter the suspension was refluxed for 1.75 h during which time the color of the solution changed from bright yellow to nearly colorless. At the end of this period, the reaction mixture was cooled to room temperature and was filtered through celite. The solvent and any remaining hydrazine were removed under reduced pressure. The crude product was then dissolved in THF and was chromatographed on basic alumina (25 g) using THF as the eluent. The eluent solvent was removed to yield air-sensitive, white crystals of **7** (1.69 g, 84.1%) that were stored under nitrogen. To prevent excessive decomposition of the aminopyridine, it was used immediately to generate the desired imine.

2-{[(2-Hydroxyphenyl)methyl]imino}-6-methylpyridin-3-ol (8): The aminopyridine **7** (1.69 g, 13.6 mmol) was dissolved in anhydrous ethanol (50 mL). Salicylaldehyde (1.66 g, 13.6 mmol) was added and the suspension was refluxed for 1 h. During this time, the color changed to red-orange and nearly all of the starting materials dissolved. The solution was allowed to cool to room temperature and the solvent was removed under reduced pressure to give a red solid. This solid was dissolved again in absolute ethanol (25 mL) and the solvent was evaporated again. This procedure was repeated twice. The solid was dissolved into boiling methanol (150 mL) and the product was crystallized by cooling to −25 °C. The product deposited as red plates which were collected by filtration and were washed with cold methanol. A second crop of the product could be obtained from the filtrate by similar treatment. Yield: 2.0 g, 64%. ^{1}H NMR (CD_2Cl_2, 20 °C, 500 MHz): $\delta=2.50$ (s, 3H), 6.91–6.95 (m, 2H), 7.06 (d, $J=8.14$ Hz, 1H), 7.25 (d, $J=6.92$ Hz, 1H), 7.45 (dd, $J_1=8.10$, $J_2=1.61$ Hz, 1H), 7.74 (d, $J=6.59$ Hz, 2H), 9.38 (s, 1H), 12.4 ppm (br. s., 1H); ^{13}C NMR ([D$_6$]DMSO, 27 °C, 125 MHz): $\delta=23.07$, 116.87, 118.93, 119.26, 123.60, 125.23, 133.17, 133.49, 143.92, 145.42, 147.00, 161.07, 161.43 ppm; ESI-MS (CD_2Cl_2): m/z: 227 [$M-1$], 228 [M]; elemental analysis calcd (%) for $C_{13}H_{12}N_2O_2$: C 68.41, H 5.30, N 12.27; found: C 68.30, H 5.33, N 12.13.

[Pt(8)DMSO] (9): A 50-mL flask was charged with [Pt(dmso)$_2$Cl$_2$] (0.925 g, 2.19 mmol) dissolved in DMSO (20 mL). K_2CO_3 (0.715 g, 5.17 mmol) and **8** (0.5 g, 2.19 mmol) were added and the mixture was heated to 140 °C. The reaction mixture was stirred at 140 °C for 15 min and the color changed to red-brown. The reaction mixture was then allowed to cool to 90 °C and distilled water (25 mL) was slowly added, precipitating the product. The mixture was stirred for 15 min and was then poured into distilled water (100 mL). The reaction mixture was stirred until it had cooled to room temperature. The crude product was isolated by filtration and was washed well with distilled water (2×25 mL). The impure yellow solid was dried, and then was dissolved in hot ethyl acetate (500 mL) and was passed through a filter frit. This solution was then chromatographed on basic alumina (20 g) using ethyl acetate as the eluent. The product is the only material that passes through this column. The yellow solution was concentrated to 75 mL under reduced pressure whereupon the product deposited as yellow needles. After the mixture had been cooled to −20 °C, the crystals were collected by filtration. The yellow needles of the product were washed with pentane (2×10 mL). Yield: 0.61 g, 56%. ^{1}H NMR ([D$_6$]DMSO, 27 °C, 500 MHz): $\delta=2.48$ (s, 3H), 2.54 (s, 6H), 6.87 (t, $J=6.9$ Hz, 1H), 7.00 (d, $J=8.3$ Hz, 1H), 7.25 (d, $J=8.5$ Hz, 1H), 7.34 (d, $J=8.3$ Hz, 1H), 7.54 (td, $J_1=6.8$, $J_2=1.6$ Hz, 1H), 8.03 (dd, $J_1=8.0$, $J_2=1.4$ Hz, 1H), 9.46 ppm (s, 1H); $^3J(^{195}\text{Pt}, \text{H-9.46})=29.7$ Hz; ^{13}C NMR ([D$_6$]DMSO, 27 °C, 125 MHz): $\delta=22.72$, 40.41, 117.10, 120.44, 121.26, 123.35, 125.29, 134.49, 135.55, 144.02, 146.46, 149.00, 156.93, 162.25 ppm; ESI-MS (CD_3CN): m/z: 499 [M], 500 [$M+1$]; elemental analysis calcd (%) for $C_{15}H_{16}N_2O_3PtS$: C 36.07, H 3.23, N 5.61; found: C 36.22, H 3.18, N 5.54.

[Pt(8)NH$_3$] (4): A dry 50-mL flask was charged with [Pt(**8**)DMSO] (0.200 g, 0.400 mmol) dissolved into freshly distilled CH_3CN (20 mL). Ammonia, as a 7 M solution in methanol, (6.60 mL, 46.2 mmol) was added to the yellow suspension of the DMSO complex. The reaction mixture was stirred at room temperature for 120 h, during which time the color of the yellow suspension changed to orange. Periodically, more ammonia was added to the reaction mixture. After 120 h the crystals were dissolved by increasing the volume of acetonitrile to 60 mL and heating. As this orange solution cooled, the product deposited as orange micro-

crystals. The volume of acetonitrile was reduced to approximately 7 mL and the resulting suspension was cooled to −20 °C. The orange crystals of the product were collected by filtration and were washed with cold acetonitrile (1×3 mL), diethyl ether (1×10 mL), and pentane (1×10 mL). Yield: 0.145 g, 82.4 %. ^{1}H NMR ([D$_7$]DMF, 27 °C, 500 MHz): δ = 2.54 (s, 3H), 4.96 (br. s, 3H), 6.75 (t, J = 7.7, 1H), 6.92 (d, J = 8.3, 1H), 7.05 (d, J = 8.5, 1H), 7.25 (d, J = 8.2, 1H), 7.50 (td, J_1 = 8.4, J_2 = 1.4, 1H), 7.94 (d, J_1 = 7.9, 1H), 9.57 ppm (s, 1H); ^3J (^{195}Pt, H-9.57) = 34.1 Hz; ^{13}C NMR ([D$_7$]DMF, 27 °C, 125 MHz): δ = 23.09, 116.85, 122.26, 122.99, 123.23, 125.23, 133.03, 135.19, 142.47, 143.23, 152.13, 160.05, 163.35 ppm. Λ_M(CH$_3$CN) = 1.05 Ω^{-1}cm^{2}mol^{-1}; ESI-MS (CD$_3$CN): m/z: 438 [M], 439 [M+1]; elemental analysis calcd (%) for C$_{13}$H$_{13}$N$_3$O$_2$Pt: C 35.62, H 2.99, N 9.59; found: C 35.95, H 2.98, N 9.57.

4-[3-Hydroxy-6-methylpyridin-2-yl)amino]but-3-en-2-one (11): A 200-mL flask was charged with **7** (2.01 g, 16.2 mmol) and 4-methoxy-3-buten-2-one (1.62 g, 16.2 mmol). The neat mixture was heated at 120 °C for 2 h. The flask was flushed with argon periodically. At the end of this period, any methanol that had been generated was removed under reduced pressure, yielding a black, resinous material. This was dissolved in THF (10 mL) and was filtered through silica (35 g). The solvent was removed and the resulting brown solid was slurried in diethyl ether (10 mL). The solid was recovered by filtration and was washed with ether (10 mL), ethyl acetate (5 mL), and pentane (10 mL). This yielded the product as a tan solid of sufficient purity (~95 %) for use in the next step. Yield: 1.28 g, 41.0 %. This product is air stable, but is susceptible to hydrolysis in wet solvents. ^{1}H NMR ([D$_6$]DMSO, 27 °C, 500 MHz): δ = 2.10 (s, 3H), 2.32 (s, 3H), 5.40 (d, J_1 = 8.0 Hz, 1H), 6.64 (d, J_1 = 7.9 Hz, 1H), 7.04 (d, J_1 = 7.9 Hz, 1H), 7.93 (dd, J_1 = 8.0, J_2 = 12.0 Hz, 1H), 9.91 (br. s, 1H) 11.62 ppm (d, J_1 = 12.0 Hz, 1H); ^{13}C NMR ([D$_6$]DMSO, 27 °C, 125 MHz): δ = 22.64, 29.10, 98.01, 116.77, 121.74, 138.13, 139.20, 140.35, 145.79, 197.90 ppm; ESI-MS (CH$_2$Cl$_2$): m/z: 191 [M−1], 192 [M].

[Pt(11)DMSO] (16): A dry 200-mL flask was charged with [Pt(dmso)$_2$Cl$_2$] (1.10 g, 2.6 mmol) dissolved in anhydrous DMSO (15 mL). Compound **11** (0.500 g, 2.6 mmol) and K$_2$CO$_3$ (0.850 g, 6.14 mmol) were added as solids to the yellow solution. The resulting slurry was heated to 140 °C over 15 min and was maintained at that temperature for a further 15 min, during which time the color changed to dark green. The solution was allowed to cool to room temperature and water (180 mL) was added to precipitate a yellow/green powder, which was isolated by filtration and was washed with water (3×20 mL). The dry solid was dissolved into hot ethyl acetate and was passed through basic alumina (20 g). The eluted solvent was removed under reduced pressure yielding yellow needles, which were recrystallized from hot hexanes. The solid (0.85 g, 70.3 %) was collected by filtration was washed with cold hexanes and vacuum dried. ^{1}H NMR ([D$_6$]acetone, 27 °C, 500 MHz): δ = 2.15 (s, 3H), 2.39 (s, 3H), 3.44 (s, 6H), 5.77 (d, J_1 = 6.7 Hz, 1H), 6.72 (d, J_1 = 8.2 Hz, 1H), 7.13 (d, J_1 = 8.2 Hz, 1H), 8.64 ppm (d, J_1 = 6.7 Hz, 1H); ^3J(^{195}Pt, H-8.64) = 23.3 Hz; ^{13}C NMR ([D$_6$]acetone, 27 °C, 125 MHz): δ = 23.11, 25.99, 42.11, 100.00, 120.97, 124.48, 141.22, 144.28, 151.31, 156.41, 178.13 ppm; ESI-MS (CH$_3$CN): m/z: 463 [M], 464 [M+1]; elemental analysis calcd (%) for C$_{12}$H$_{16}$N$_2$O$_3$PtS: C 31.10, H 3.48, N 6.05; found: C 31.14, H 3.44, N 5.95.

[Pt(11)NH$_3$] (3): A dry 50-mL sealable flask was charged with [Pt(**11**)DMSO] (0.150 g, 0.32 mmol) dissolved in freshly distilled CH$_3$CN (20 mL). Ammonia, as a 7 M solution in methanol, (2 mL, 14.0 mmol) was added to the yellow solution of the DMSO complex. The reaction flask was sealed and the reaction mixture was heated to 60 °C using an oil bath. The reaction mixture was stirred at this temperature for 24 h, during which time the color changed to light orange. At the end of this period, the reaction mixture was allowed to cool and was then transferred to a 100-mL flask. The solvent was removed under reduced pressure yielding a yellow powder. The compound was recrystallized by vapor diffusion of diethyl ether into a CH$_3$CN solution of the product. The yellow needles (0.121 g, 92.0 %) were collected by filtration and were washed with cold CH$_3$CN (3 mL), diethyl ether (5 mL), and pentane (5 mL). ^{1}H NMR ([D$_6$]acetone, 27 °C, 500 MHz): δ = 1.86 (s, 3H), 2.35 (s, 3H), 4.31 (br. s, 3H), 5.52 (d, J = 6.5 Hz, 1H), 6.62 (d, J = 8.1 Hz, 1H), 7.01 (d, J = 8.1 Hz, 1H), 8.58 ppm (d, J = 6.5 Hz, 1H); ^3J(^{195}Pt, H-8.58) = 32.5 Hz; ^{13}C NMR ([D$_6$]acetone, 27 °C, 125 MHz): δ = 23.12, 25.76, 99.74, 120.12, 123.63, 137.53, 142.50, 153.65, 158.11, 174.27 ppm; Λ_M (CH$_3$CN) = 1.36 Ω^{-1}cm^{2}mol^{-1}; ESI-MS (CH$_3$CN): m/z: 402 [M], 403 [M+1]; elemental analysis calcd (%) for C$_{10}$H$_{13}$N$_3$O$_2$Pt: C 29.85, H 3.26, N 10.44; found: C 29.85, H 3.40, N 10.47.

[(2-Hydroxyphenyl)amino]but-3-en-2-one (17): A 50-mL flask was flame-dried and was flushed with argon. The flask was charged with the 4-methoxy-3-buten-2-one (0.5 g, 4.99 mmol) dissolved in THF (10 mL). This yellow solution was cooled to −10 °C and *o*-aminophenol (0.545 g, 4.99 mmol) dissolved in THF (7 mL) was added. The reaction mixture was stirred at −10 °C for 2.5 h and was then allowed to warm to room temperature. The reaction mixture was stirred at room temperature for 2 h. The solvent was removed under reduced pressure to yield a yellow solid. This solid was recrystallized from a minimum amount of hot THF by cooling to −20 °C. The crystals were collected by filtration and were washed with ethyl acetate (5 mL) and hexanes (5 mL). This yielded a yellow powder of sufficient purity (~97 %) for the next step. Yield: 0.445 g, 50.3 %. ^{1}H NMR ([D$_6$]DMSO, 16 °C, 500 MHz): δ = 2.03 (s, 3H), 5.30 (d, J = 7.70 Hz, 1H), 6.77–6.84 (m, 4H), 7.31 (d, J = 7.75 Hz, 1H), 7.58 (dd, J_1 = 12.8, J_2 = 7.60 Hz, 1H), 10.02 (br. s, 1H), 11.53 (d, J = 12.8 Hz, 1H); ^{13}C NMR ([D$_6$]DMSO, 27 °C, 125 MHz): δ = 29.75, 97.59, 113.85, 115.81, 120.26, 123.43, 129.07, 142.77, 145.97, 197.53 ppm; ESI-MS (CD$_2$Cl$_2$): m/z: 177 [M], 178 [M+1].

[Pt(17)DMSO] (18): A 100-mL flask was charged with [Pt(dmso)$_2$Cl$_2$] (0.477 g, 1.13 mmol) dissolved into DMSO (8 mL). K$_2$CO$_3$ (0.477 g, 1.13 mmol) and **17** (0.2 g, 1.13 mmol) were added and the slurry was heated to 140 °C. The slurry was stirred at 140 °C for 15 min as the color changed to yellow-brown. The reaction mixture was then allowed to cool to 90 °C and distilled water (23 mL) was slowly added, precipitating the product. This suspension was stirred for 15 min and was then poured into distilled water (80 mL). The mixture was stirred until it had cooled to room temperature. The crude product was isolated by filtration and was washed well with distilled water (2×25 mL). The yellow solid was dried and was then dissolved into hot ethyl acetate and passed through a filter frit. This solution was then chromatographed on basic alumina (8 g) using ethyl acetate as the eluent. The product is the only material that passes through this column. The yellow eluent solution was concentrated to a small volume under reduced pressure. The product deposited as yellow needles on the sides of the flask. The product was completely precipitated by addition of ether. It was collected by filtration (0.435 g, 86.0 %). ^{1}H NMR ([D$_6$]acetone, 27 °C, 500 MHz): δ = 2.12 (s, 3H), 3.30 (s, 6H), 5.65 (d, J = 6.6 Hz, 1H), 6.57–6.60 (m, 1H), 6.87–6.93 (m, 2H), 7.70 (d, J = 7.9 Hz, 1H), 8.18 ppm (d, J = 6.6 Hz, 1H); ^3J(^{195}Pt, H-8.18) = 25.4 Hz; ^{13}C NMR ([D$_6$]acetone, 27 °C, 125 MHz): δ = 25.77, 42.23, 99.46, 114.92, 116.58, 117.97, 126.83, 140.40, 141.78, 166.12, 175.55 ppm; ESI-MS (CD$_3$CN): m/z: 448 [M], 449 [M+1]; elemental analysis calcd (%) for C$_{12}$H$_{15}$NO$_3$PtS: C 32.14, H 3.37, N 3.12; found: C 32.41, H 3.44, N 3.04.

[Pt(17)NH$_3$] (5): A dry 50-mL sealable flask was charged with [Pt(**17**)DMSO] (0.150 g, 0.335 mmol) dissolved into freshly distilled CH$_3$CN (10 mL). Ammonia, as a 7 M solution in methanol, (1.5 mL, 10.5 mmol) was added to the yellow suspension of the DMSO complex. The flask was sealed and the temperature was elevated to 60 °C. The reaction mixture was stirred at this temperature for 24 h. The volume of acetonitrile was then reduced to 5 mL and the product was crystallized from the solution by vapor diffusion with ether. The orange crystals of the product were collected by filtration and were washed with diethyl ether (5 mL) and pentane (1×10 mL). Yield: 0.090 g, 69 %. ^{1}H NMR ([D$_6$]acetone, 27 °C, 500 MHz): δ = 1.86 (s, 3H), 4.30 (br. s, 3H), 5.42 (d, J = 6.3 Hz, 1H), 6.47–6.50 (m, 1H), 6.79–6.85 (m, 2H), 7.64 (d, J = 8.1 Hz, 1H), 8.09 ppm (d, J = 6.3 Hz, 1H); ^3J(^{195}Pt, H-8.09) = 30.6 Hz; ^{13}C NMR ([D$_6$]acetone, 27 °C, 125 MHz): δ = 25.37, 99.01, 114.85, 117.24, 125.82, 137.47, 141.54, 167.82, 171.57 ppm; Λ_M(CH$_3$CN) = 1.12 Ω^{-1}cm^{2}mol^{-1}; ESI-MS (CD$_3$CN): m/z: 387 [M], 388 [M+1]; elemental analysis calcd (%) for C$_{10}$H$_{12}$N$_2$O$_2$PtS: C 31.01, H 3.12, N 7.23; found: C 31.32, H 2.98, N 7.27.

Host–guest interaction of 1 with 3: A series of 2.00 mM solutions of **1** in dry CD$_3$CN containing varying amounts of **3**, ranging from 0.46 mM to 10.96 mM, were prepared and were examined by ^{1}H NMR spectroscopy (70 °C). The host in CD$_3$CN solution is yellow, as is the guest. The host–guest mixtures vary in color from pale orange to deep red. The mole ratio method[16] was applied, and the stoichiometry of the association was found to be 1:1 (supporting information). The maximum chemical shift change for any of the protons of the host was $\Delta\delta$ = 0.6 ppm (H$_b$). Several other protons of the host had maximum chemical shift changes in the

range, $\Delta\delta = 0.25$ to 0.6 ppm. The maximum chemical shift change observed for the guest was $\Delta\delta = 1.07$ ppm, several other protons had chemical shifts changes of about $\Delta\delta = 0.51$ to 1.02 ppm. The data were analyzed by using a curve fitting procedure[9] and $K_{1,3}$ was found to be $21000 \pm 4000\,M^{-1}$; ESI-MS (CD_3CN): m/z: 609.5 $[H-2PF_6]^{2+}$, 810.0 $[HG-2PF_6]^{2+}$ (see Supporting Information).

Host–guest interaction of 1 with 4: The host–guest association constant for **1** and **4** in CD_3CN solution at 70 °C was determined by the ^1H NMR titration method described for the association of **1** and **3**. A series of 2.00 mM solutions of **1** in dry CD_3CN containing varying amounts of **4**, ranging from 0.53 mM to 13.9 mM, were used. The data were analyzed using a curve fitting procedure[9] and $K_{1,4}$ was found to be $37000 \pm 6000\,M^{-1}$; ESI-MS (CD_3CN): m/z: 608.6 $[H-2PF_6]^{2+}$, 828.0 $[HG-2PF_6]^{2+}$ (see Supporting Information).

Titration of 3 with trifluoroacetic acid (TFA): A series of 0.477 mM solutions of **3** in dry CD_3CN containing varying amounts of dry TFA, ranging from 0.927 mM to 38.9 mM, were prepared and were examined by absorption spectrometry (25 °C). The guest **3** in CD_3CN solution is yellow, and TFA is colorless. The acid–base mixtures vary in color from yellow to orange (Figure 5). The protonation of **3** was also studied by using ^1H NMR spectroscopy (70 °C). A series of 2.15 mM solutions of **3** in dry CD_3CN containing varying amounts of dry TFA, ranging from 1.30 mM to 198 mM, were prepared. The data was consistent with the results obtained by UV/Vis spectroscopy (see Supporting Information).

Titration of the host–guest complex derived from 1 and 3 with trifluoroacetic acid: A series of solutions containing 2.00 mM of **1** and 2.00 mM of **3** in dry CH_3CN containing varying amounts of TFA, ranging from 4.62 mM to 191 mM, were prepared. These solutions were examined by absorption spectrometry at 25 °C giving the results shown in Figure 7. The protonation of the host–guest complex, formed by 2.00 mM each of **1** and **3** was also monitored by ^1H NMR spectroscopy at 70 °C in CD_3CN in the presence of TFA ranging from 0.64 mM to 199 mM. Plots of the change in chemical shift ($\Delta\delta$) verses equivalents of TFA, obtained from the ^1H NMR data (70 °C) were again consistent with the results obtained by UV/Vis spectroscopy (see Supporting Information).

Titration of 4 with trifluoroacetic acid: A series of 0.456 mM solutions of **4** in dry CD_3CN containing varying amounts of TFA, ranging from 0.608 mM to 77.9 mM, were prepared and were examined by absorption spectrometry. The change in absorbance ($|\Delta A|$) was plotted against the equivalents of TFA (supporting information). This plot indicated that 60 equivalents of TFA are required to fully protonate **4**. The protonation of **4** was also studied by using ^1H NMR spectroscopy (70 °C). A series of 2.15 mM solutions of **4** in dry CD_3CN containing varying amounts of TFA, ranging from 1.30 mM to 260 mM, were prepared and examined by ^1H NMR spectroscopy. The data were consistent with the results obtained by UV/Vis spectroscopy (see Supporting Information).

Titration of the host–guest complex derived from 1 and 4 with trifluoroacetic acid: These experiments were carried out in analogous way to that described for TFA addition to the host–guest complex formed by **1** and **3**. The degree of dissociation was monitored by UV/Vis spectroscopy at 25 °C and by ^1H NMR spectroscopy at 70 °C in CD_3CN solutions (see Supporting Information).

Crystallographic structural determination for 5: X-ray quality crystals of **5** were grown by cooling a hot saturated solution of the complex in acetonitrile. Data collection: A needle-shaped crystal ($0.68 \times 0.08 \times 0.06$ mm) was selected under a stereo-microscope while immersed in Fluorolube oil. The crystal was removed from the oil using a tapered glass fiber that also served to hold the crystal for data collection. The crystal was mounted and centered on a Bruker SMART APEX system at 100 K. Rotation and still images showed many of the diffractions to be sharp, however, a few diffractions appeared doubled or amorphous on some frames. Frames separated in reciprocal space were obtained and provided an orientation matrix and initial cell parameters. Final cell parameters were obtained from the full data set. A "hemisphere" data set was obtained which samples approximately 1.2 hemispheres of reciprocal space to a resolution of 0.84 Å using 0.3° steps in ω using 20 s integration times for each frame. Data collection was made at 100 K. Integration of intensities and refinement of cell parameters were done using SAINT.[28] Absorption corrections were applied using SADABS[28] based on redundant diffractions. Structure solution and refinement: The space group was determined as $P2_1/c$ based on systematic absences and intensity statistics. Patterson methods were used to locate the Pt atom. Repeated difference Fourier maps allowed recognition of all expected C, O, and N atoms. Following anisotropic refinement of all atoms, ideal H atom positions were calculated. No anomalous bond lengths or thermal parameters were noted.

Crystallographic structural determination for 1: X-ray quality crystals of the complex **1** were grown by slow evaporation of a −20 °C acetonitrile solution of the complex over two years. The yellow diamonds that result are very fragile and they effloresce, and were stored in the mother liquor. The small crystal size, weak diffractions, and ready loss of solvent necessitated data collection using synchrotron radiation. Data collection: A fragment of a yellow, diamond shaped crystal ($0.07 \times 0.04 \times 0.015$ mm) was selected under a polarizing microscope while immersed in Fluorolube oil to avoid possible loss of solvents of crystallization. The crystal was removed from the oil using a tapered glass fiber that also served to hold the crystal for data collection. The crystal was mounted and centered on a goniometer with Kappa geometry at ChemMatCARS Sector 15 beamline at the Advanced Photon Source at Argonne National Laboratory. The sample was cooled to 100 K. Still images showed the diffractions to be sharp. Data collection consisted of 1220 frames separated by 0.3 degree rotations in phi with the detector to sample distance set to 4 cm. Integration time for each frame was 2 s. The unit cell was obtained by using SMART and integration of intensities and refinement of cell parameters were done using SAINT.[28] Absorption corrections were applied using SADABS[28] based on redundant diffractions. Structure solution and refinement: The space group was determined as $P\bar{1}$ based on systematic absences and intensity statistics. Patterson methods were used to locate the Pd atoms as well as P and Cl atoms. Repeated difference Fourier maps allowed recognition of all expected C, N, and F atoms. Five acetonitrile molecules were also located in the asymmetric unit. Hydrogen atom positions were calculated. Final refinement was anisotropic for all non-hydrogen atoms and isotropic for H atoms. No anomalous bond lengths were noted although a few displacement ellipsoids were elongated, possibly due to disorder in *tert*-butyl groups.

Crystallographic structural determination for the host–guest complex formed from 1 and 3: Crystals of the complex were grown by dissolving a 1:1 mixture of the host **1** and guest **3** in methyl ethyl ketone and vapor diffusing with methanol for seven days, at −4 °C. Data collection: A red diamond ($0.40 \times 0.40 \times 0.45$ mm) was selected under a stereo-microscope while immersed in Fluorolube oil to avoid possible loss of solvent. The crystal was removed from the oil using a tapered glass fiber that also served to hold the crystal for data collection. The crystal was mounted and centered on a Bruker SMART APEX system at 100 K. Rotation and still images showed the diffractions to be sharp. Frames separated in reciprocal space were obtained and provided an orientation matrix and initial cell parameters. Final cell parameters were obtained from the full data set.

A full sphere data set was obtained using 0.3° steps in ω using 30 s integration times for each frame. Data collection was made at 100 K. Integration of intensities and refinement of cell parameters were done using SAINT[28]. Absorption corrections were applied by using SADABS[28] based on redundant diffractions.

Structure solution and refinement: The space group was determined as $P\bar{1}$ based on systematic absences and intensity statistics. Patterson methods were used to locate the Pt atom, the Pd atoms, and the P atoms. Repeated difference Fourier maps allowed recognition of all expected C, N, and Cl atoms located on the host (C(1)–C(65), N(1)–N(7), and Cl(1) and Cl(2)). The atoms on the host molecule were located with ease and following anisotropic refinement of these atoms, the ideal H atom positions were calculated. The bond distances and angles of the atoms associated with the host are unremarkable and no unusual thermal ellipsoids were noted. Refinement of the occupancy of the P atoms located by Patterson methods revealed one of the P atoms to be of single occupancy and two to be of one-half occupancy. Repeated difference Fourier maps allowed recognition of the F atoms associated with these P atoms. The PF_6 ion of 100% occupancy was refined aniostropically. The F atom octahedra of the two one-half occupancy PF_6 ions share a face and the P and F atoms of these one-half occupancy ions were refined isotropically. The guest is disordered over two positions in approximately a 7:3 ratio determined by examination of C atom occupancy. The Pt atom and immediate coordina-

tion sphere (N(8), N(9), O(1), and O(2)) of the two orientations of the guest appear to be superimposed. That is, the two orientations of the guest appear to be related by rotation about the line defined by N(8)-Pt(1)-N(9). The C and (pyridine) N atoms of the two orientations of the guest were located with difficulty by comparison of a Fourier contour map of the electron density of this plane with the positions that would be predicted from the crystal structure of **5**. The occupancy of these C and N atoms has been refined. The C and (pyridine) N atoms associated with the 70% occupancy isomer are C(66)–C(75) and N(10) and those associated with the 30% occupancy isomer are C(76)–C(83) and N(11). The Pt atom and the atoms of the immediate coordination sphere (N(8), N(9), O(1), and O(2)) were refined anisotropically. The carbon and nitrogen atoms of the remaining portion of the ligand were refined isotropically and the H atoms associated with the ligand of the guest were not calculated. The bond distances and angles between Pt(1) and (N(8), N(9), O(1), and O(2) are near expected values. Because of the two-site disorder and near superpositioning of many of the remaining atoms of the guest, the bond distances and angles of the remaining portion of the guest are distorted from expected values. Two methanol molecules were located in the structure, one of 70% occupancy, the other 100% occupancy. One 70% occupancy acetonitrile molecule was also located. These solvent molecules were refined isotropically and the H atom positions were not calculated. In addition to these well-defined solvent molecules two regions of unidentifiable but structured electron density were located in the E-map. These were assigned as C atoms (C(94)–C(98) and C(88)–C(93) and C(99)) and the occupancy refined. The locations and occupancies of these atoms suggest that they are associated with disordered solvent. In addition to these semi-structure locations of electron density in the E-map a number of unstructured single points of electron density were located in the E-map. SQUEEZE was implemented to remove these remaining points of electron density and 61 electrons were removed using this routine. A check of the "cif" file for this structure revealed the possibility of higher symmetry (*C*2/*c*). Solution of the structure in *C*2/*c*, however, led to less satisfactory results.

CCDC-221482 (**1**), CCDC-221481 (**5**), and CCDC-221483 (**1·3)** contain the supplementary crystallographic data for this paper. These data can be obtained free of charge via www.ccdc.ac.uk/conts/retrieving.html (or from the Cambridge Crystallographic Data Centre, 12 Union Road, Cambridge CB2 1EZ, UK; Fax: (+44) 1223-336-033; or e-mail: deposit@ccdc.cam.ac.uk).

Acknowledgement

This work was supported by the Basic Energy Sciences Division, Department of Energy. Argonne National Laboratories are thanked for access to the CARS facility. ChemMatCARS Sector 15 is principally supported by the National Science Foundation/Department of Energy under grant numbers CHE9522232 and CHE0087817 and by the Illinois board of higher education. The Advanced Photon Source is supported by the U.S. Department of Energy, Basic Energy Sciences, Office of Science, under Contract No. W-31–109-Eng-38.

[1] *Molecular Switches* (Ed.: B. L. Feringa), Wiley-VCH, Weinheim, **2001**.

[2] a) M. Schliwa, G. Woehlke, *Nature* **2003**, *422*, 759–765; b) A. Houdusse, H. L. Sweeney, *Curr. Opin. Struct. Biol.* **2001**, *11*, 182–194; c) A. F. Huxley, *Phil. Trans. R. Soc. Lond. B.* **2000**, *355*, 433–440; d) F. J. Kull, S. A. Endow, *J. Cell Sci.* **2002**, *115*, 15–23; e) D. Stock, A. G. Leslie, J. E. Walker, *Science* **1999**, *286*, 1700–1705.

[3] a) M. Yoshida, E. Muneyuki, T. Hisabori, *Nat. Rev. Mol. Cell Biol.* **2001**, *2*, 669–677; b) G. Oster, H. Wang, *Biochim. Biophys. Acta* **2000**, *1458*, 482–510; c) P. D. Boyer, *Annu. Rev. Biochem.* **1997**, *66*, 717–749; d) P. Dimroth, *Biochim. Biophys. Acta* **2000**, *1458*, 374–386.

[4] a) T. C. Elston, G. Oster, *Biophys. J.* **1997**, *73*, 703–721; b) S. C. Schuster, S. Khan, *Annu. Rev. Biophys. Biomol. Struct.* **1994**, *23*, 509–539; c) H. C. Berg, *Philos. Trans. R. Soc. London. Ser. B.* **2000**, *355*, 491–501; d) D. J. Derosier, *Cell* **1998**, *93*, 17–20.

[5] a) V. Balzani, A. Credi, F. M. Raymo, J. F. Stoddart, *Angew. Chem.* **2000**, *112*, 3484–3531; *Angew. Chem. Int. Ed.* **2000**, *39*, 3348–3391; b) V. Balzani, A. Credi, *Chem. Rec.* **2001**, *1*, 422–435; c) M. C. Jimenez-Molero, C. Dietrich-Buchecker, J. -P. Sauvage, *Chem. Commun.* **2003**, *14*, 1613–1616; d) B. X. Colasson, C. Dietrich-Buchecker, M. C. Jimenez-Molero, J. -P. Sauvage, *J. Phys. Org. Chem.* **2002**, *15*, 476–483.

[6] a) R. A. Bissel, E. Córdova, A. E. Kaifer, J. F. Stoddart, *Nature* **1994**, *369*, 133–137; b) M. Asakawa, P. R. Ashton, V. Balzani, A. Credi, C. Hamers, G. Mattersteig, M. Montalti, A. N. Shipway, N. Spencer, J. F. Stoddart, M. S. Tolley, M. Venturi, A. J. P. White, D. J. Williams, *Angew. Chem.* **1998**, *110, 357–361; Angew. Chem. Int. Ed. Engl.* **1998**, *37*, 333–337.

[7] a) F. Ibukuro, T. Kusukawa, M. Fujita, *J. Am. Chem. Soc.* **1998**, *120*, 8561–8562; b) W-Y. Sun, T. Kusukawa, M. Fujita, *J. Am. Chem. Soc.* **2002**, *124*, 11 570–11 571.

[8] A. J. Goshe, I. M. Steele, C. Ceccarelli, A. L. Rheingold, B. Bosnich, *Proc. Natl. Acad. Sci. USA* **2002**, *99*, 4823–4829.

[9] a) A. J. Goshe, I. M. Steele, B. Bosnich, *J. Am. Chem. Soc.* **2003**, *125*, 444–451; b) R. D. Sommer, A. L. Rheingold, A. J. Goshe, B. Bosnich, *J. Am. Chem. Soc.* **2001**, *123*, 3940–3952.

[10] a) *Extended Linear Chain Compounds, Vols. 1–3* (Ed.: J. S. Miller), Plenum, New York, **1982–1983**; b) J. R. Miller, *J. Chem. Soc.* **1965**, 713–720; c) K. Krogmann, *Angew. Chem.* **1969**, *81*, 10–17; *Angew. Chem. Int. Ed. Engl.* **1969**, *8*, 35–42; d) V. H. Houlding, V. M. Miskowski, *Coord. Chem. Rev.* **1991**, *111*, 145; e) W. B. Connick, R. E. Marsh, W. P. Schaefer, H. B. Gray, *Inorg. Chem.* **1997**, *36*, 913–922; f) W. B. Connick, L. M. Henling, R. E. Marsh, H. B. Gray, *Inorg. Chem.* **1996**, *35*, 6261–6265.

[11] G. A. Barclay, B. F. Hoskins, *J. Chem. Soc.* **1965**, 1979–1991.

[12] a) J. A. Bailey, M. G. Hill, R. E. Marsh, V. M. Miskowski, W. P. Schaefer, H. B. Gray, *Inorg. Chem.* **1995**, *34*, 4591–4599; b) J. A. Bailey, V. M. Miskowski, H. B. Gray, *Inorg. Chem.* **1993**, *32*, 369–370; c) M. G. Hill, J. A. Bailey, V. M. Miskowski, H. B. Gray, *Inorg. Chem.* **1996**, *35*, 4585–4590.

[13] W. J. Geary, *Coord. Chem. Rev.* **1971**, *7*, 81–122.

[14] B. H. Han, D. H. Shin, S. Y. Cho, *Tetrahedron. Lett.* **1985**, *26*, 6233–6224.

[15] H. Motschi, C. Nussbaumer, P. S. Pregosin, F. Bachechi, P. Mura, L. Zambonelli, *Helv. Chim. Acta* **1980**, *63*, 2071–2086.

[16] a) A. S. Meyer, G. H. Ayres, *J. Am. Chem. Soc.* **1957**, *79*, 49–53; b) H. -J. Schneider, *Principles and Methods in Supramolecular Chemistry*, Wiley, New York, **2000**.

[17] a) V. Rudiger, H. -J. Schneider, *Chem. Eur. J.* **2000**, *6*, 3771–3776; b) S. Simova, H. -J. Schneider, *J. Chem. Soc. Perkin Trans. 2* **2000**, 1717–1722.

[18] K. Izutsu, *Acid-Base Dissociation Constants in Dipolar Aprotic Solvents*, Blackwell, London, **1990**.

[19] A. R. Katritzky, D. E. Leahy, *J. Chem. Soc. Perkin Trans. 2* **1983**, 45–48.

[20] a) G. Weber, S. A. Anderson, *Biochemistry* **1965**, *4*, 1942–1947; b) W. B. Person, *J. Am. Chem. Soc.* **1965**, *87*, 167–170; c) D. A. Deranleau, *J. Am. Chem. Soc.* **1969**, *91*, 4044–4049; d) L. Fielding, *Tetrahedron* **2000**, *56*, 6151–6170.

[21] a) G. Oster, H. Wang, *Trends Cell Biol.* **2001**, *11*, 196–202; b) G. Oster, H. Wang, *Appl. Phys. A* **2002**, *75*, 315–323.

[22] P. Reimann, *Phys. Rep.* **2002**, *361*, 57–265.

[23] a) W. Jiang, J. Hermolin, R. H. Fillingame, *Proc. Natl. Acad. Sci. USA* **2001**, *98*, 4966–4971; b) D. Stock, A. G. Leslie, J. E. Walker, *Science* **1999**, *286*, 1700–1705; c) H. Seelert, A. Poetsch, N. A. Dencher, A. Engel, H. Stahlberg, D. J. Müller, *Nature* **2000**, *405*, 418–419; d) H. Stahlberg, D. J. Müller, K. Suda, D. Fotiadis, A. Engel, T. Meier, U. Matthey, P. Dimroth, *EMBO Rep.* **2001**, *2*, 229–233.

[24] a) T. Elston, H. Wang, G. Oster, *Nature* **1998**, *391*, 510–513; b) G. Oster, H. Wang, *Structure* **1999**, *7*, R67-R72.

[25] Molecular machines special issue (Ed.: J. F. Stoddart),*Acc. Chem. Res.* **2001**, *34*, 409–522.

[26] a) D. A. Leigh, J. K. Y. Wong, F. Dehez, F. Zerbetto, *Nature* **2003**, *424*, 174–179; b) A. M. Brouwer, C. Frochot, F. G. Gatti, D. A. Leigh, L. Mottier, F. Paolucci, S. Roffia, G. W. Wurpel, *Science* **2001**,

291, 2124 – 2128; c) N. Koumura, R. W. J. Zijistra, R. A. Van Delden, N. Harada, B. L. Feringa, *Nature* **1999**, *401*, 152 – 155.
[27] R. Romeo, L. M. Scolaro, *Inorg. Synth.* **1998**, *32*, 153 – 158.
[28] G. Sheldrick, SHELXTL (version 6.1) program library; G. Bruker Analytical X-ray Systems, Madison, WI, **2000**.

Received: October 14, 2003
Revised: January 19, 2004 [F5620]

